HUGHES RESEARCH LABORATORIES
Malibu, California

a division of hughes aircraft company

Ready

DESIGN AND CONSTRUCTION OF AMMONIA BEAM MASER

J. L. Walsh

Technical Summary Report
Contract No. NASw-62
April 1962

TABLE OF CONTENTS

LIST OF ILLUSTRATIONS

ABSTRACT

13558

This report describes the construction of two ammonia beam masers and associated frequency translators which demonstrate, under laboratory conditions, a long term frequency stability of better than one part in 10^{10}. The masers utilize two critically coupled cavities[1] in order to minimize frequency pulling effects due to cavity drift. The cavities are separated by 9/4 wavelengths and are both tuned to the maser frequency. This configuration produces a minimum phase shift (due to cavity drift, etc.) of the resonant cavity system as seen by the ammonia beam. The masers incorporate a point source and tapered focuser[2] and operate with $N^{15}H_3$ derived from a chemical source, which affords excellent beam stability. Associated with each maser is a frequency translator consisting of a 52.7 Mc crystal, whose output is multiplied and phase locked to the maser output, thus providing signals with maser stability at frequencies in a more useful part of the r-f spectrum.

Author

I. INTRODUCTION

The objective of this program was the development of two laboratory model ammonia beam masers with their associated frequency translating circuitry which would operate with a stability of one part in 10^{10} over a period of one week. This requirement arose out of consideration of both the general and special relativistic effects on a satellite traveling in an orbit about the earth. Theoretical predictions of these effects are shown in Fig. 1. From these curves, we see that the effects are of opposite sign. The special theory of relativity predicts that a clock in a satellite will run slow compared with a clock on the surface of the earth and that the effect will be maximum at the surface of the earth. The general theory of relativity predicts that a clock in a satellite will run faster than a clock on the surface of the earth, the effect increasing with altitude. The net contribution of these two effects cancels at an orbit radius of 1.5 earth radii. It is seen from the curves that in order to obtain significant experimental data, the clocks, both on the ground and in orbit, should have stabilities of better than one part in 10^{10}.

The ammonia beam maser offers certain advantages over other devices proposed for this same application: namely, the cesium beam frequency standard and the optically pumped rubidium gas cell. The ammonia maser is the only active source among these three. The other two devices behave like very-stable, very-high-Q band-pass filters. In frequency standard applications, these devices are driven by a signal with much lower stability, and a servo-feedback loop is provided to maintain this signal at the center of their respective pass bands. Short term stability is thus limited by the time constants of the feedback circuit, which is of the order of seconds. The ammonia maser offers further advantages in that there are no complicated alignment problems and that its whole structure is basically both rugged and simple.

Although the recently developed atomic hydrogen maser has demonstrated higher stabilities than those contemplated here, it seems a rather unlikely candidate for satellite application, for the time being at least, because of the fragile nature of some of the components and the relatively large magnet required.

Two separate ammonia beam masers, each equipped with double cavities, have been constructed under this contract. A block diagram of the entire system is shown in Fig. 2 and a photograph is shown in Fig. 3. Each maser contains two liquid-nitrogen-filled cold traps, one inside the maser chamber itself and the second between the maser chamber and the diffusion pump. These cold traps are attached to a system which maintains their liquid-nitrogen level automatically for a period of at least 12 hours so that they can operate unattended. With this arrangement, the masers can operate for an almost indefinite period of time. The focuser voltage required for each of the masers is supplied from a common high voltage power supply whose output is

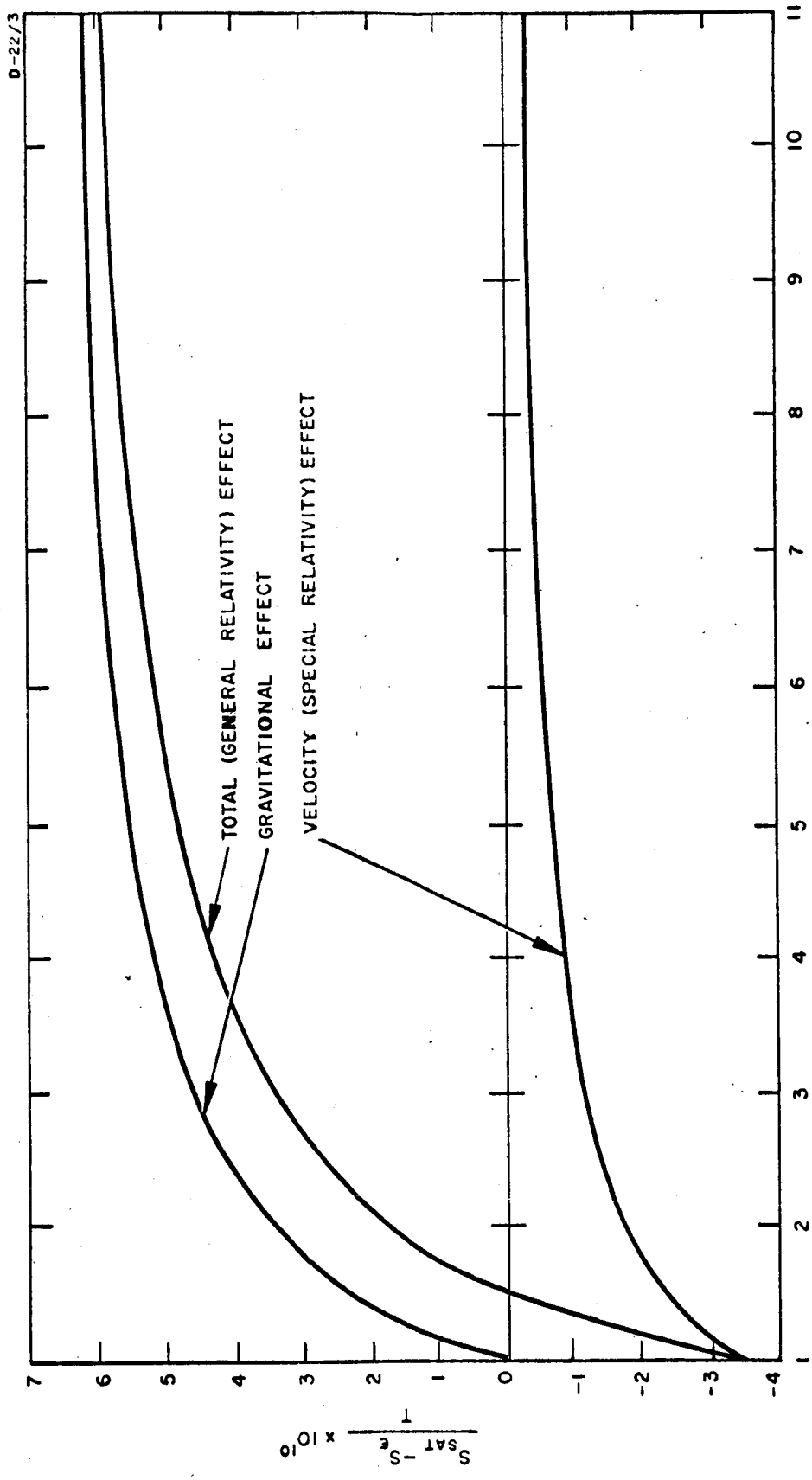

Fig. 1. Time dilatational effects experienced by clock in satellite relative to a clock on the ground.

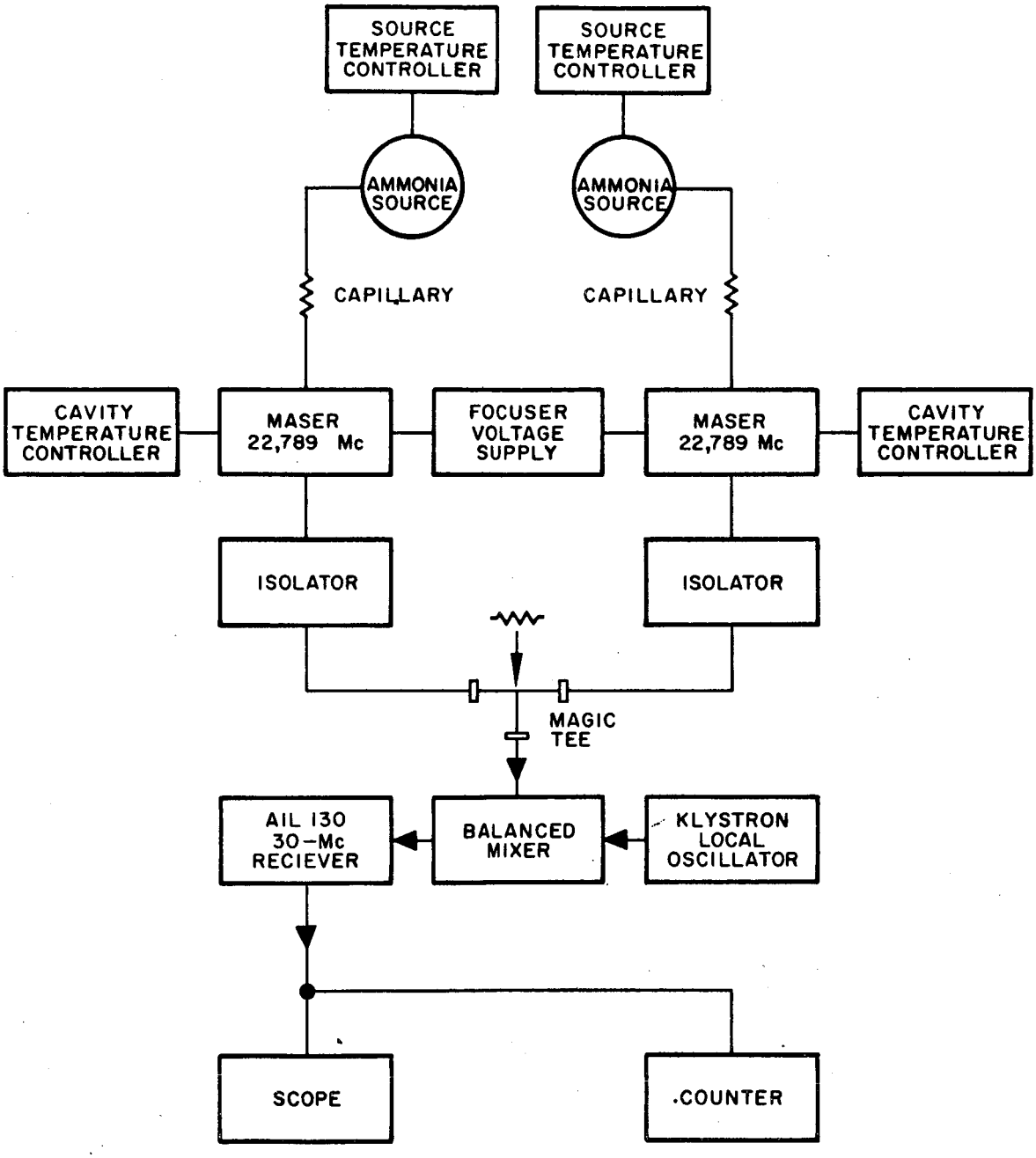

Fig. 2. Block diagram of ammonia maser system.

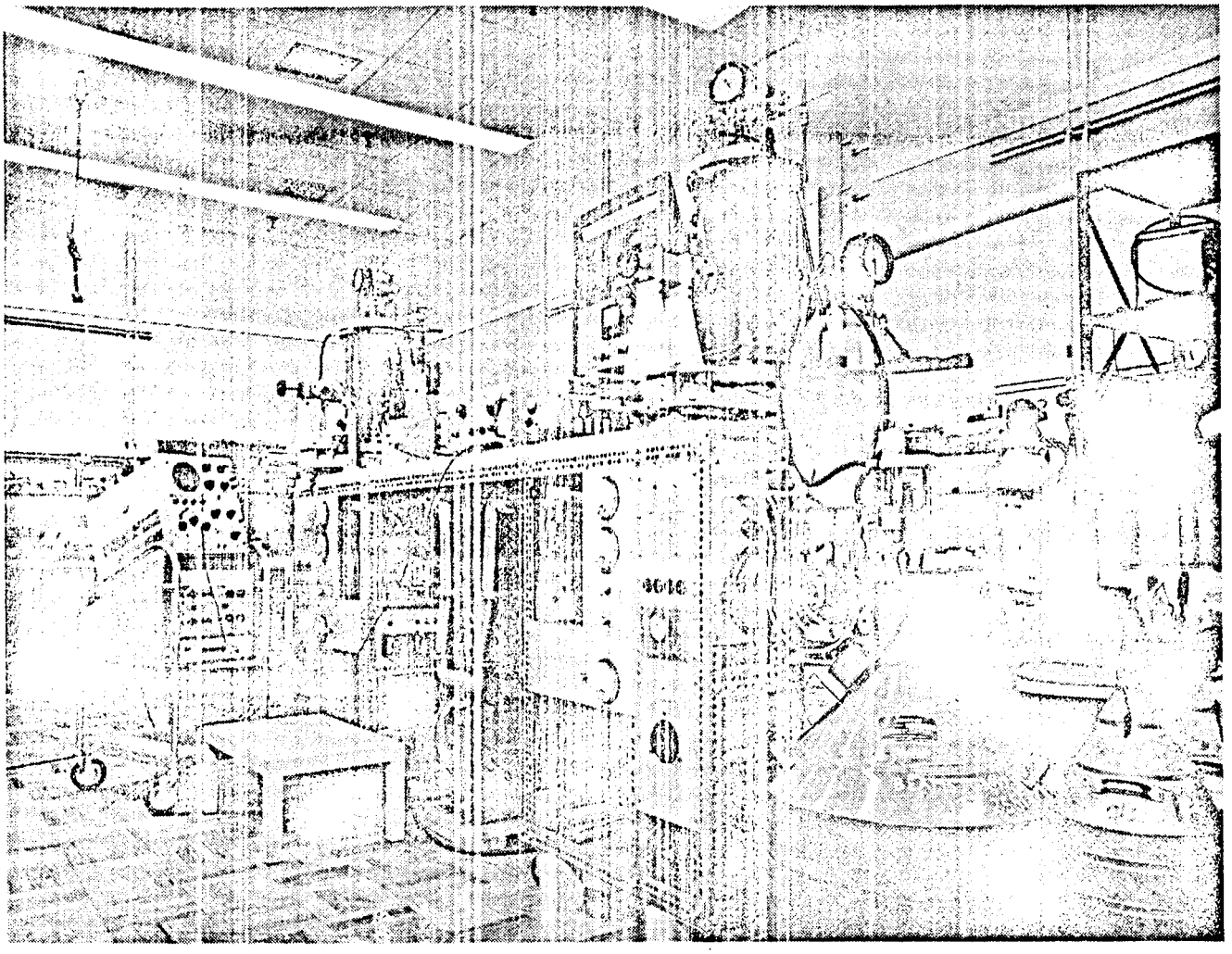

Fig. 3. Ammonia maser clock system.

balanced to ground. Provision is made for the recovery of the $N^{15}H_3$ after it has passed through the maser. Our tests with $N^{14}H_3$ indicate that a recovery in excess of 96 percent is possible. Two complete, fully transistorized, phase-locked tracking loops have also been constructed as part of each maser system. These phase-locked loops permit us to obtain signals with the same frequency stability as the maser, but at higher power and in a more useful part of the r-f spectrum.

II. SIMPLIFIED THEORY OF AMMONIA BEAM MASER OPERATION

Before beginning our discussion of the ammonia beam maser, we consider first the ammonia molecule itself. The ammonia molecule is tetrahedral in shape, with the three hydrogen atoms at the corners of an equilateral triangle and the nitrogen atom at the apex of the tetrahedron. One possible mode of vibration of this molecule is an oscillatory motion of the nitrogen atom through the plane of the hydrogen atoms, which is referred to as an inversion transition. It occurs at a frequency of 23,870.11 Mc for $N^{14}H_3$ and 22,789.41 Mc for $N^{15}H_3$. The ammonia molecule, however, can be accurately explained only in quantum mechanical terms. We think of the molecule in terms of its energy levels, with an oscillation of the sort mentioned above viewed as a transition between two of these energy levels. We are concerned in particular with the rotational state known as J = 3, K = 3, where J and K are rotational quantum numbers, and we wish to consider the inversion transition for this rotational state. To understand the operation of the ammonia beam maser, consider the two levels between which the inversion transition takes place.

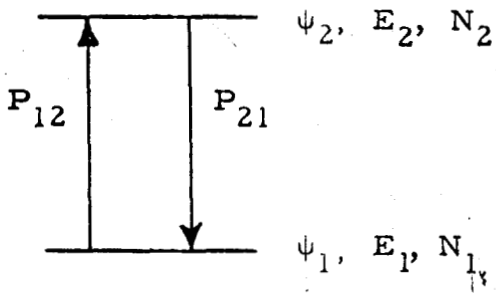

Let us label the lower state as state 1 and the upper state as state 2. Associated with each of these states are wave functions ψ_1 and ψ_2 and energies E_1 and E_2, respectively. We consider first the probability of transitions between these two states, and we denote by P_{12} the probability per unit time per molecule of a transition taking place between state 1 and state 2 when radiation at frequency $\nu_{21} = (E_2 - E_1)/h$ is supplied to the system. In like manner, we can consider P_{21} the probability that a transition takes place between state 2 and state 1 when radiation is applied at the same frequency. It can be shown from quantum mechanical

considerations that these two probabilities are equal. P_{12} is the probability of absorption per atom per unit time and P_{21} is the probability for stimulated emission per atom per unit time.

We must now consider the relative populations of these two states under conditions of thermal equilibrium. It can be shown on thermodynamical grounds that if we have a sample of gas in thermal equilibrium at some absolute temperature T, the relative numbers of molecules in state 1 and state 2 will be given by

$$N_1 = Ce^{-E_1/kT} \qquad N_2 = Ce^{-E_2/kT}.$$

In the case of ammonia, about 3 percent of the total number of molecules is in each one of these rotational states in thermal equilibrium at room temperature. Thus, since the number of molecules in thermal equilibrium in the lower energy state is greater than that in the upper state by about one part in 250 and since, as we have seen above, the transition probabilities per molecule up and down are equal, we shall have, upon application of radiation to this system, absorption at the transition frequency. If, however, we can upset thermal equilibrium in such a way that the number of molecules in the upper state is greater than that in the lower state, then upon application of radiation to the system, the system will give up energy to the radiation field and amplification may occur. This process is referred to as maser action, maser being an acronym for Molecular Amplification by the Stimulated Emission of Radiation.

In the case of the ammonia beam maser, this reversal of population, i.e., the increase in the number of molecules in state 2 over state 1, is accomplished by means of a focuser. This focuser consists of four circular rods arranged around the periphery of a circle as shown in Fig. 4. Alternate rods are connected together and to a source of high d-c potential. Thus, we find a high field between adjacent electrodes as shown with zero electric field in the center.

The action of the focuser can be described as follows. Ammonia molecules are injected approximately down the axis of the focuser by the source with a thermal velocity at room temperature of 6×10^4 cm/sec. Most of the molecules will have a small radial component of velocity tending to move them off the axis of the focuser, in spite of the fact that the source offers rather good collimation. Thus, most of the molecules will find themselves drifting into the electric field between the focuser electrodes as they leave the source, and it is this fact that we depend upon for operation of the focuser. Since the ammonia molecule is essentially nonpolar, the electric field induces in the molecule an electric dipole moment; this induced moment, in turn, interacts with the electric

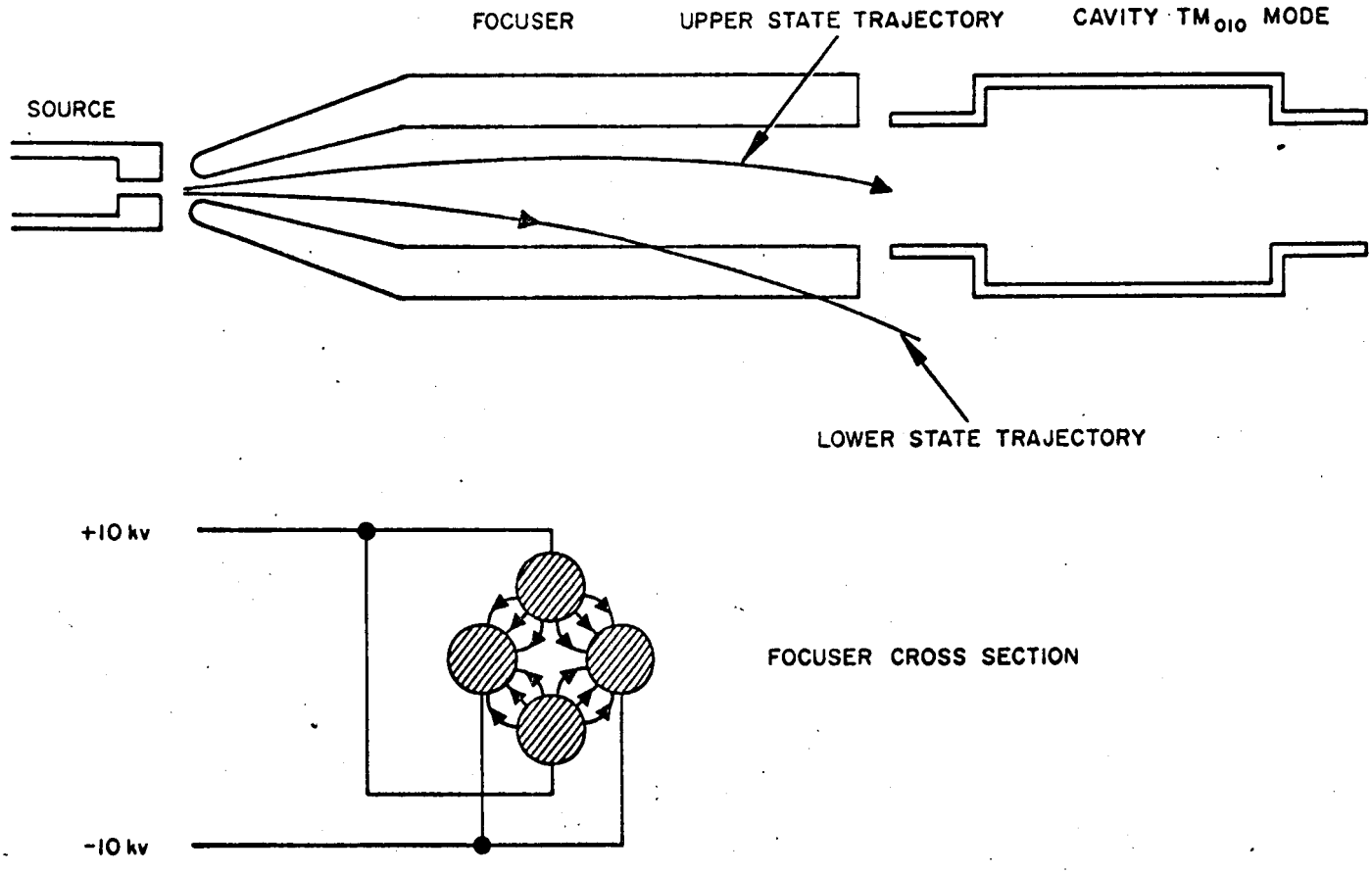

Fig. 4. Schematic diagram of the elements of an ammonia beam maser.

field to produce an energy of the configuration proportional to the square of the electric field. Thus we can write $W = CE^2$, where C is a proportionality constant. On the basis of quantum mechanical analysis, we find that the constant C is positive for the upper state and negative for the lower state. Since this energy is in the nature of a potential energy, molecules having a small radial component of velocity (as essentially all of them do) which are injected down the axis of the focuser by the source will be returned to the axis of the focuser if they are in the upper state and, at the same time, tend to be removed from the axis of the focuser, if they are in the lower state. By this means the focuser removes most of the lower state molecules from the beam; however, only about 6 percent of the upper state molecules are actually focused and maintained on the axis of the focuser. The molecules which have been focused then enter the microwave cavity operating in a TM_{010} mode with short sections of cylindrical waveguide beyond cutoff open at the ends, as shown in Fig. 4. Thus, the cavity has a relatively large mechanical opening, but is still an electrically closed configuration.

III. OPERATING CONDITIONS

The power output available from an ammonia beam maser is of the order of 10^{-10} to 10^{-11} watt. The spectral purity is a small fraction of 1 cps. In order for operation as described above to take place, we must maintain a high vacuum within the maser so that the mean free paths of the ammonia molecules will be long compared with the dimensions of the maser. A pressure of 10^{-6} mm is used since the mean free path of ammonia molecules is of the order of 40 meters at this level. Furthermore, since the influx of ammonia is rather high, of the order of 10^{17} to 10^{18} molecules/sec, a very high pumping speed for ammonia is required. The masers utilize liquid-nitrogen cold traps located inside the maser chamber which have a very high pumping speed for ammonia, since it has been estimated that an ammonia molecule striking a liquid-nitrogen surface has approximately a 50-percent probability for sticking.

IV. FREQUENCY STABILITY

There are a large number of factors influencing the stability of the ammonia maser. The biggest single factor is cavity pulling. Two resonant systems coupled together produce an output frequency different from that of the molecule. In our case, the resonant circuit of the ammonia molecule itself is coupled to the resonant circuit of the microwave cavity. The output frequency ν of such a combination can be expressed approximately as follows:

$$\nu = \nu_o + \frac{Q_C}{Q_M} (\nu_C - \nu_o),$$

where

$\nu_o \equiv$ natural molecular frequency

$\nu_C \equiv$ cavity resonant frequency

Q_C and $Q_M \equiv$ cavity and molecular Q's, respectively.

Typically $Q_C/Q_M = 10^{-3}$ so that $\nu = \nu_o + 10^{-3}(\nu_C - \nu_o)$. We see, therefore, that the cavity resonant frequencies must be controlled quite closely. For a stability of one part in 10^{10}, we require the cavity to be stable to within approximately 2-1/2 kc at K-band. If, however, we make use of two cavities critically coupled together so that the response of the combined cavity system is as shown below, the requirements for frequency control of the individual cavities are relaxed considerably, as shown in Table I.

Single Cavity

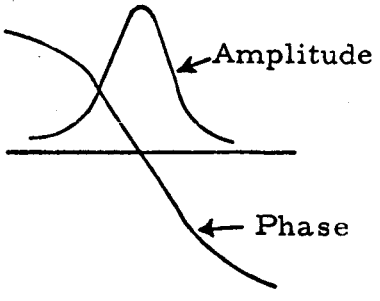

Double Cavity

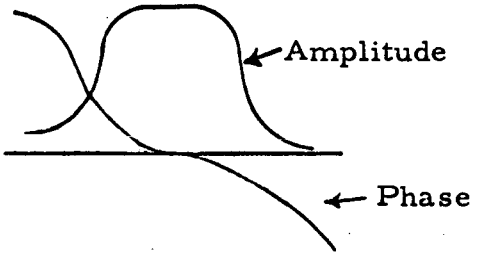

TABLE I

Maximum Allowable Cavity Frequency and Temperature Shifts for Copper Cavities to Maintain a Stability in Maser Output Frequency of One Part in 10^{11}

	Allowable Cavity Frequency Shift, cps	Corresponding Temperature Shift for Copper, ^{o}C	Corresponding Axial Motion of Tuning Probe, inches
Single cavity	250	0.0007	2×10^{-6}
Twin cavity	10^{5}	0.26	7×10^{-4}
Twin cavity with 1.05 VSWR into second cavity	10^{4}	0.026	7×10^{-5}
Twin cavity with 0.002 error in guide wavelength	10^{5}	0.26	7×10^{-4}
Twin cavity with 0.020 error in guide wavelength	3×10^{4}	0.078	2×10^{-4}

As part of this effort, extensive work was carried out with ceramics and super-invar cavities. It was determined that for maser purposes, the best results could be obtained with cavities made of copper. Some of the factors involved in this consideration are as follows: (1) super-invar has the disadvantage of being a magnetic shielding material, thereby making it difficult, if not impossible, to tune the masers by use of the Zeeman effect. (2) Cavities made with extremely low temperature coefficient ceramic materials, while having considerably relaxed temperature regulation requirements, have poor thermal conductivity, thus making the temperature control problem more difficult. (3) Because the tuning of these cavities by means of movable probes is possible over only a somewhat limited range, it is desirable to have the possibility of additional thermal tuning; therefore, it is necessary to use a material with some reasonable value for its thermal expansion coefficient, such as copper.

As we mentioned above, the effect of cavity pulling is by far the largest single factor to be considered in the frequency stability of the ammonia maser. It is possible, for example, for a cavity to pull the output frequency of the ammonia maser as much as a few kilocycles before the maser goes out of operation, which corresponds to a frequency change of one part in 10^7. There are a number of other factors, however, which must be considered when the stabilities desired are of the order of several parts in 10^{11}.

The next two significant factors to be considered are the effects of ammonia beam flux variation and the effects of focuser voltage variation. Both of these effects are alleviated by the use of ammonia $N^{15}H_3$ instead of the conventional ammonia $N^{14}H_3$. Typical values are shown below:

For frequency stability of one part in 10^{11},

	$N^{14}H_3$	$N^{15}H_3$
Allowable beam flux variation	0.3%	10%
Allowable focuser voltage variation	0.1%	0.7%

The reason for the improvement in the case of $N^{15}H_3$ is that the N^{14} nucleus has an electric quadrupole moment which gives rise to three lines separated by about 3 kc. The oscillation taking place is a composite of these three lines. The amplitude of each of these lines may vary somewhat with the focuser voltage and beam flux and as a result give rise to wider excursions than would be expected from a single line. In the case of N^{15}, the nuclear electric quadrupole moment is zero and so we have only one line. A photograph of the maser is shown in Fig. 5.

M 1781

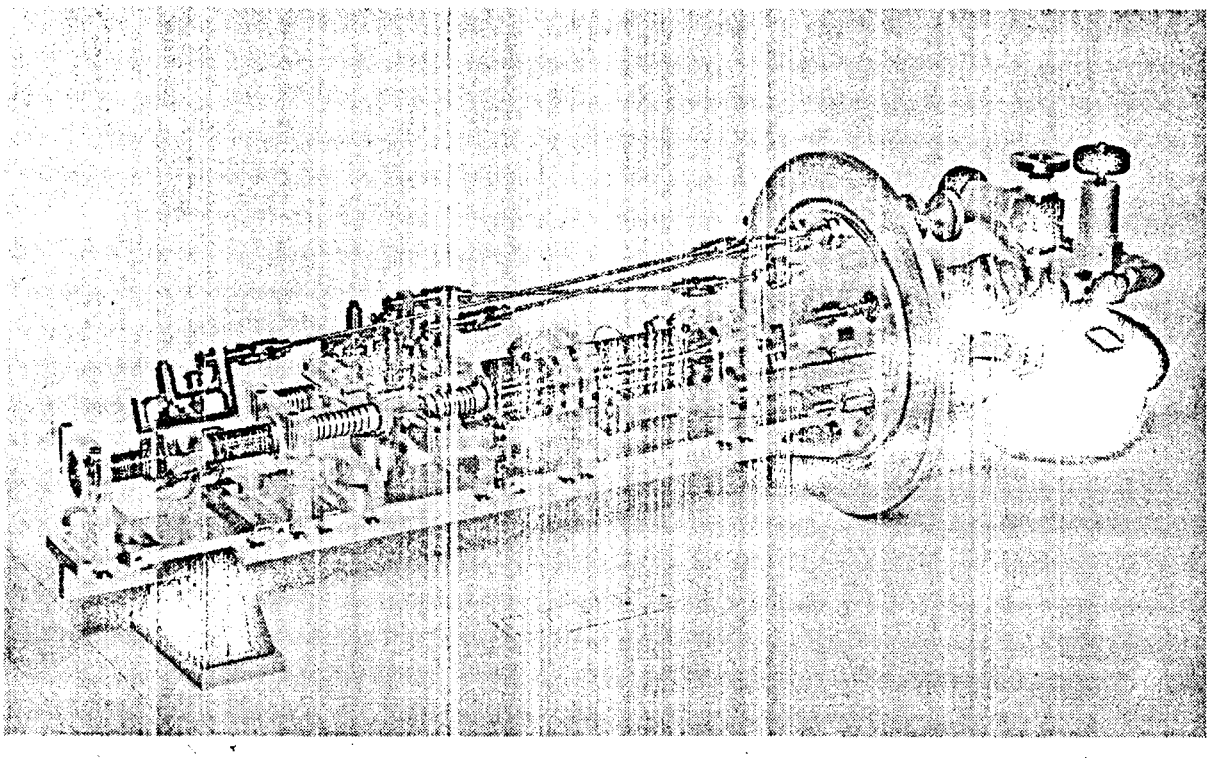

Fig. 5. Ammonia beam maser showing the nozzle focuser and double cavity. A third cavity located downstream from the double cavity is also shown.

V. MASER DESIGN CONSIDERATIONS

A. Focuser Design

The focuser is of the four-pole tapered variety which has been described by Helmer, et al.[2] The electrodes are 8 inches long and constructed of highly polished stainless steel. They are mounted on four lucite supports and carefully positioned for accurate alignment. The source consists of a single-hole 4-mil-diameter nozzle approximately 15 mils long. The separation of the source and focuser is not particularly critical in this maser. These units operate with a separation of about 3/32 of an inch. It is not necessary to cool the focuser electrodes as has been done by a number of workers since the cylindrical cold trap around the inside of the maser chamber provides more than adequate pumping speed for the ammonia gas used in this system. The diameter of the focusing electrodes is 0.060 inch at the source end, increasing to 0.300 inch at the cavity end of the focuser. These focusers are operated typically with 18 kv between adjacent electrodes.

B. Cavity Design

The resonant cavity system constitutes one of the most critical parts of the maser. As mentioned earlier, one has the choice between an extremely low temperature coefficient ceramic or invar materials and copper, which has a relatively higher coefficient of thermal expansion. The design philosophy for the cavity system may be summarized as follows:

1. Double cavities are desirable even for extremely low temperature coefficient materials for the following reasons:

   a. The requirements on dimensional stability – things relating to creep and relaxation of stresses in fabrication – are considerably reduced.

   b. Even a monomolecular layer of diffusion pump oil or some other material deposited on the inside surface of a single cavity could have considerable effect upon the frequency stability. If one makes use of a double cavity however, where the cavity stability requirements are considerably relaxed, the effects of such a deposit would be enormously reduced.

2. Once we recognize the requirement for double cavities, based on the above considerations, we see that even for copper the temperature control requirements for a stability of one part in 10^{11} are not overly stringent. When we consider this together with the many advantages to be gained from using copper, it is quite apparent that it is by far the best material for cavity construction. Some of these advantages might be enumerated as follows:

a. It is possible to machine aluminum mandrels with both a very high degree of surface finish and a very tight dimensional control, the outside dimensions of these mandrels conforming to the required inside dimensions of the finished copper cavities, to then electrodeposit copper over the aluminum mandrels, etch out the aluminum mandrel after the electrodeposition, and wind up with a microwave cavity, the inside dimensions and finish of which correspond extremely closely to those of the aluminum mandrel. Needless to say, it is much easier to machine to high tolerance and polish the outside contour of a mandrel than to hold the same tolerance and finish on an inside dimension. For this reason, it is much easier to fabricate and hold dimensions on the electrodeposited copper cavities, especially where a large number are required as in this case.

b. The copper is deposited in an almost stress-free condition so that the problem of creep should be almost nonexistent with this type of fabrication.

Each of the cavities is 4 inches in inside length and is operated in the TM_{010} mode. The design considerations relating to the choice of cavity inside diameters are shown in Fig. 6. The fabrication tolerance on the inside diameter of the cavity is ± 0.0001 inch, which corresponds to a frequency change of 5.6 Mc at the transition frequency for $N^{15}H_3$, 22,789.41 Mc. For our purposes, this is a rather large frequency tolerance, but it corresponds to the tightest practicable dimensional tolerance on the aluminum mandrels.

There are two methods of fine tuning of the resulting cavities. The first of these, which is a fixed adjustment, comes about by our choice of the temperature at which we shall control the operation of the cavity. With copper cavities operating at the temperature under consideration, we can tune approximately 0.4 Mc/°C change in cavity temperature. The second method of tuning the cavities is by means of an adjustable precision probe inserted into the center of the cavities. This probe may be either copper, when it is desired to increase the

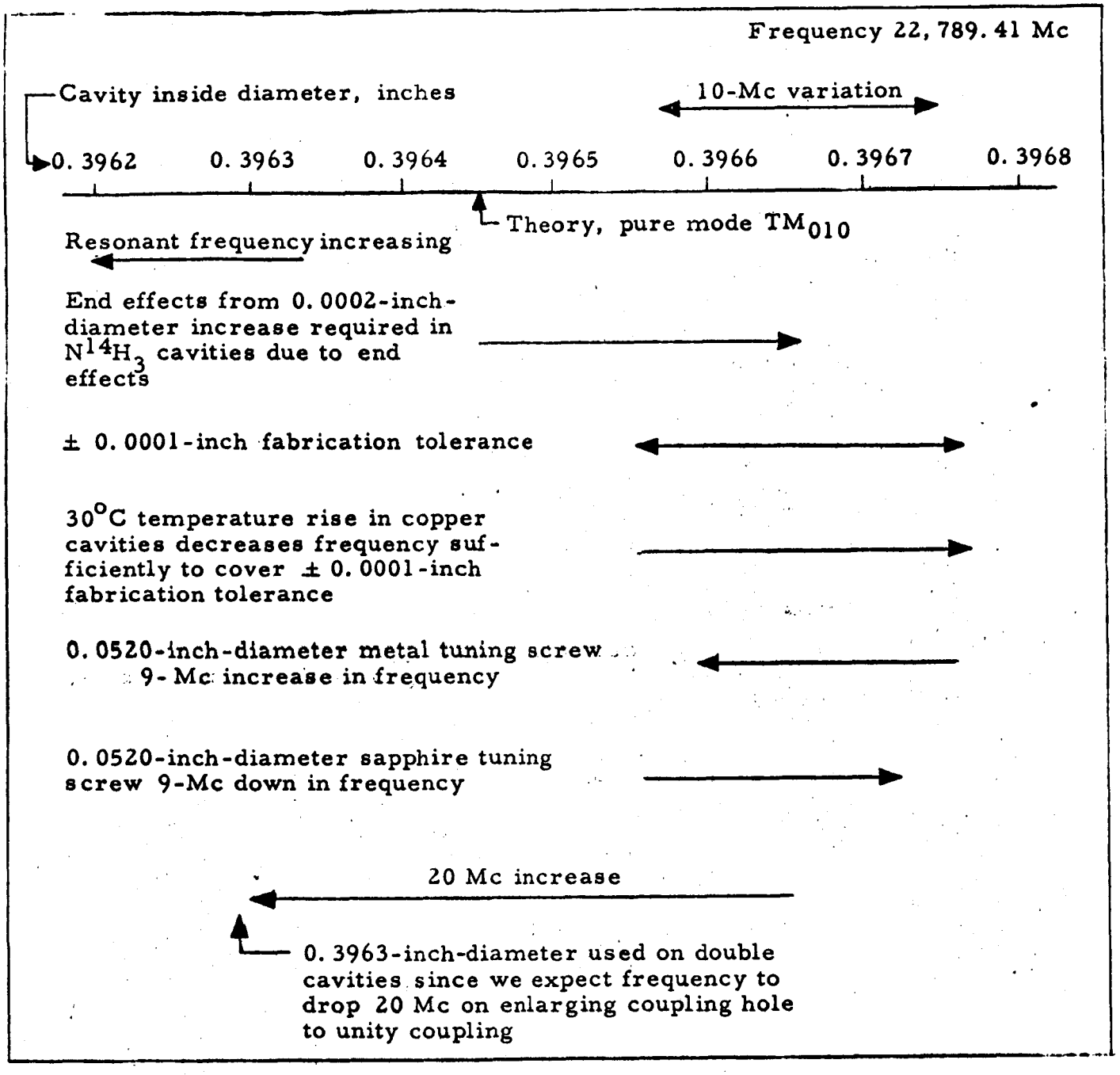

Fig. 6. $N^{15}H_3$ maser cavity design considerations.

frequency of the cavity with probe insertion, or sapphire, when it is desired to decrease the frequency of the cavity as the probe is inserted. Both of these materials have an effective tuning range of about 9 Mc without appreciable Q deterioration. The probes are driven by a precision gear and micrometer drive arrangement from outside the maser chamber. With this arrangement, it is possible to position the probe penetration into the cavity within about thirty millionths of an inch and thereby set the cavity frequency within about 5 kc. This is sufficient to obtain a frequency stability due to cavity setting in excess of one part in 10^{11}.

The layout of the maser cavity system is shown in Fig. 7. Each of the double cavities is adjusted so that the standing-wave ratio at resonance looking into the cavity is less than 1.05. The cavity in the ammonia beam has, in addition, a small sampling hole attached to an output waveguide to make possible the observation of the double-cavity system characteristics. This hole is considerably undercoupled, the standing-wave ratio looking into it being greater than 70. Adjustment of the critical coupling holes requires a diameter tolerance on the coupling hole of approximately 0.0001 inch. The actual size required was arrived at by a trial-and-error procedure consisting of measurement of the standing-wave ratio on a precision standing-wave indicator, removal of the cavity, and enlargement of the coupling hole as required in a precision jig borer. Standing-wave ratio at resonance was then plotted as a function of coupling-hole diameter, and from these data the required coupling-hole size could be determined. A typical plot is shown in Fig. 8.

The standing-wave-ratio variation with probe insertion is also shown in Fig. 8. It will be noted that it is possible to find a coupling-hole size such that the standing-wave ratio is less than 1.05 for all positions of the tuning probe. The probe is driven into the cavity by a precision micrometer drive acting on a ruby sphere which in turn rests in a small pocket in the head of each probe. This arrangement results in a very smooth minimum friction drive. The probes are returned to their original position by means of a small coil spring which acts against the micrometer drive. A diagram of the arrangement is shown in Fig. 9.

In order to maintain the low standing-wave ratio required in the $7/4\ \lambda_g$ waveguide between the double cavities, careful attention must be paid to possible reflections at the flanged joint. A K-band waveguide fabricated to commercial tolerances (± 0.002 inch on inside dimensions) could produce, under the worst conditions, an SWR of 1.04 at the joint. By using specially selected sections of silver waveguide which were available, we were able to maintain tolerances of less than ± 0.0005 inch in the mating waveguide sections and thereby obtain an SWR < 1.01 due to the flanged joint.

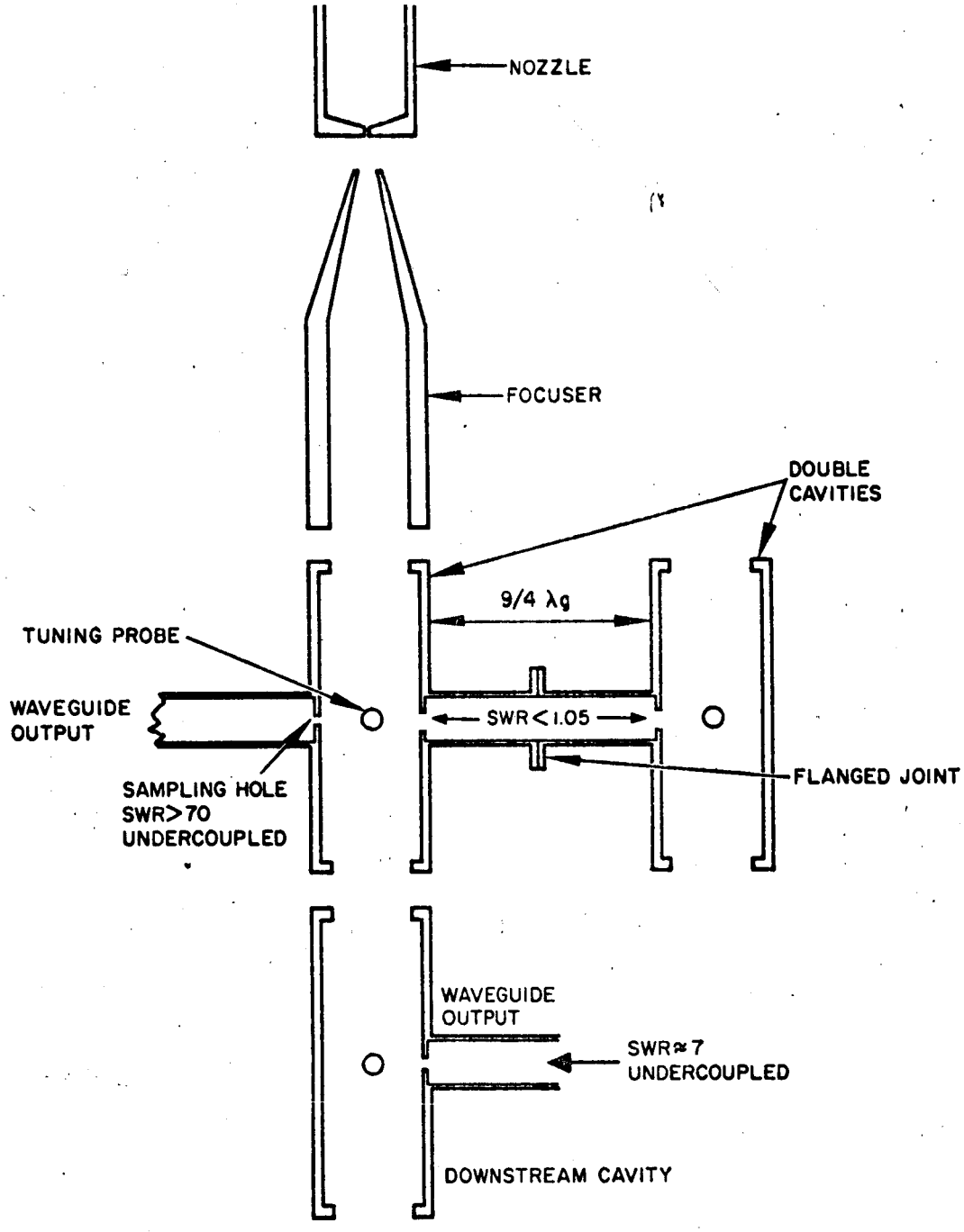

Fig. 7. Schematic diagram of the ammonia maser with double cavity.

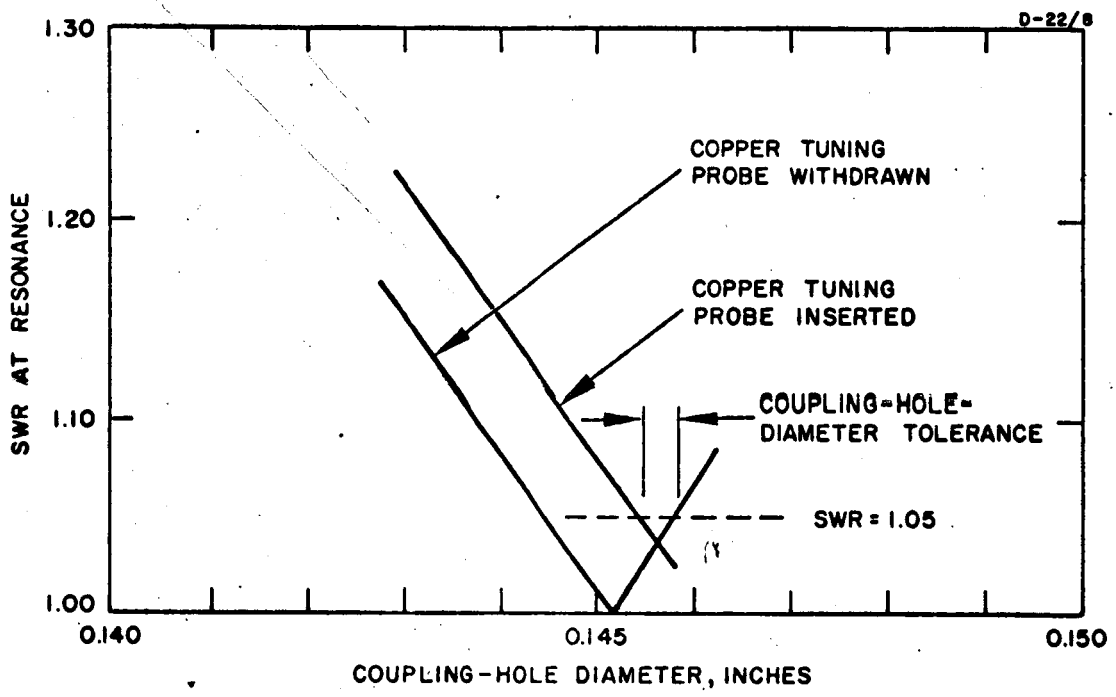

Fig. 8. Standing-wave ratio at resonance as a function of coupling-hole size.

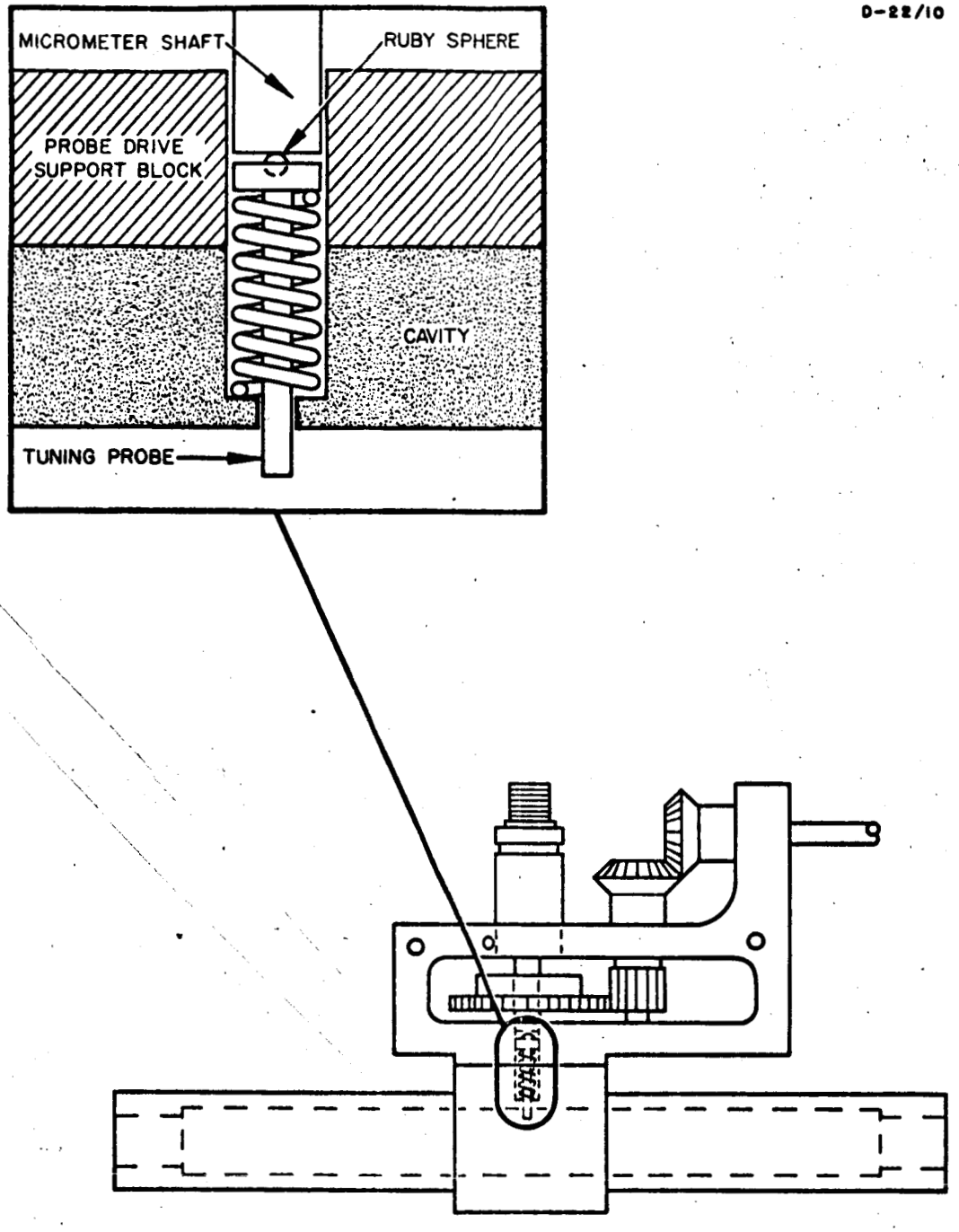

Fig. 9. Tuning mechanism of the maser cavities. Probe is driven into cavity by a micrometer shaft driving small ruby sphere which rests in a small pocket in the head of the probe. The drive is against a small spring shown.

Each cavity is wound with a coil of platinum resistance wire and a noninductive heater winding closely coupled together. The platinum resistance thermometer winding forms one arm of a Wheatstone bridge. The three resistors in the other arms of the bridge are located inside the vacuum chamber immediately adjacent to the cavity. The bridge is driven at very low power by an external oscillator at approximately 1000 cycles. The signal from the Wheatstone bridge is amplified by a very high gain amplifier, sent to a phase sensitive detector so that it can be determined whether the bridge is out of balance (too hot or too cold), and appropriate heating currents applied. The cavity temperature controllers, shown in Fig. 10, have been fully transistorized and maintain the cavity temperature within several hundredths of a degree Centigrade over extended periods. A photograph of the double-cavity configuration with the attached tuning mechanism is shown in Fig. 11.

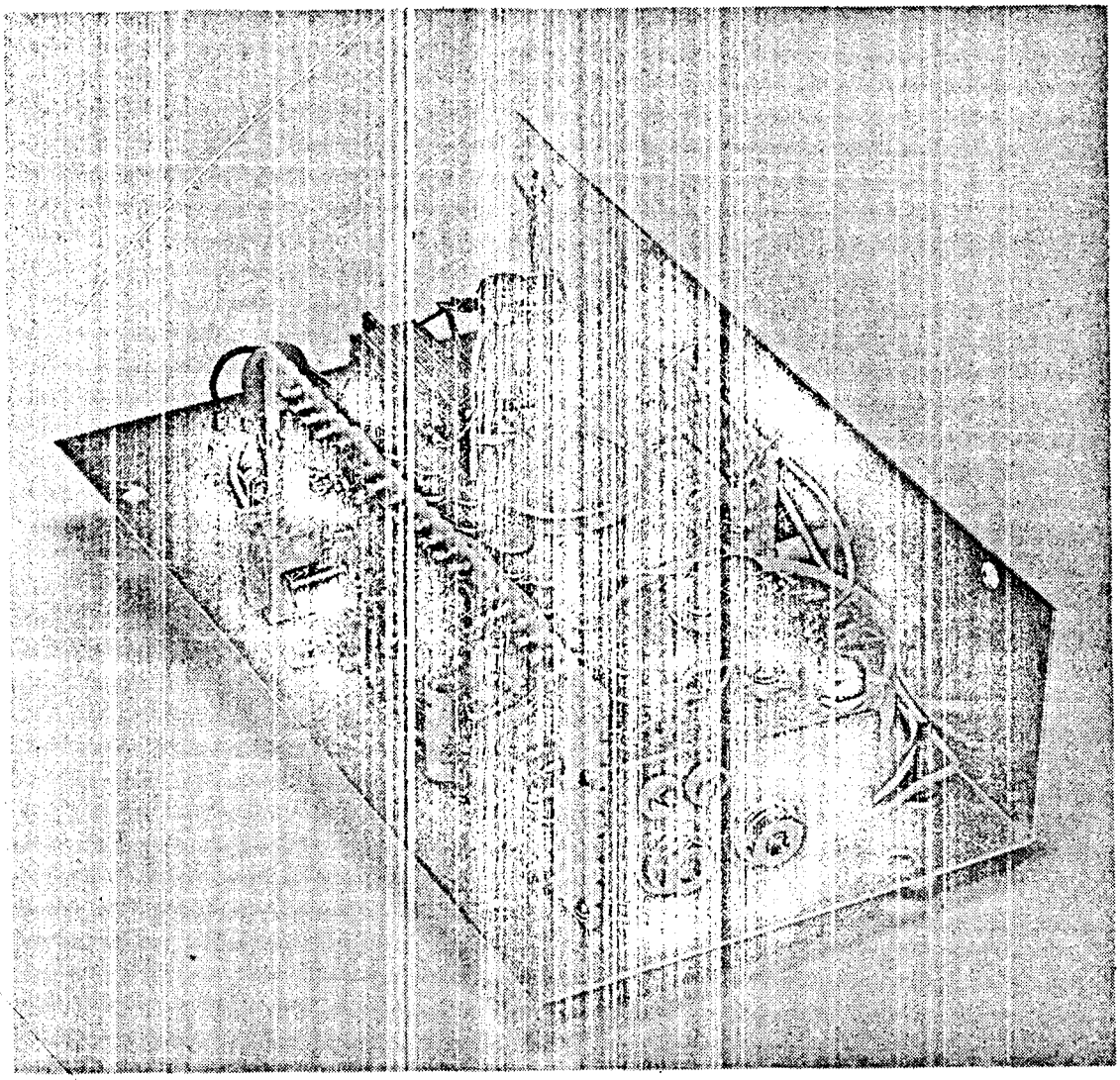

Fig. 10. Transistorized cavity temperature controller.

M 1935

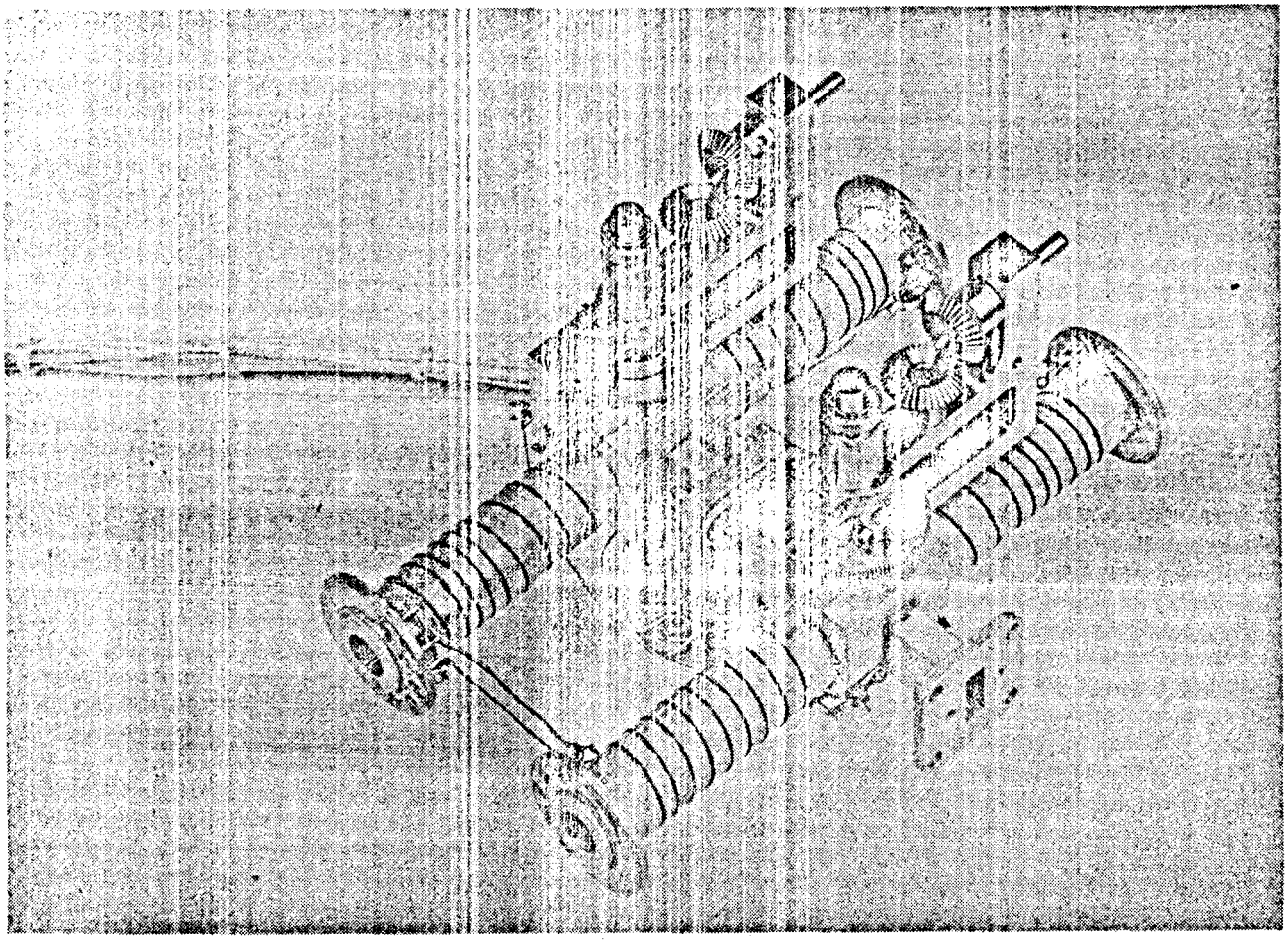

Fig. 11. The double-cavity configuration, showing temperature control windings. The tuning drive mechanisms are in place.

VI. AMMONIA CHEMICAL SOURCE

As discussed earlier, one of the requirements for the stable operation of the ammonia beam maser is that the rate of entry of ammonia molecules into the maser be held constant within certain limits. Bearing in mind the possible eventual use of this maser in a satellite, it becomes desirable to use an ammonia source which requires no elaborate pressure-regulating hardware and a minimum of temperature control in order to maintain the beam flux constant within the required limits. Since the weight of the final package should be held to a minimum, it is preferable to use a low-molecular-weight solid, which can release essentially all of the expensive $N^{15}H_3$ ($450 per gram) without experiencing a decrease in pressure at a given temperature. Liquid ammonia in equilibrium with its vapor is ruled out as a potential source since its high vapor pressure (of the order of 10 atmospheres at room temperature) requires that it be stored in a massive, heavy-walled steel container. Furthermore, in a spinning, tumbling satellite, one could not eliminate the possibility of both phases being in contact with the flow-regulating device, whereas with a solid, the two phases could be separated easily by placing over the source material a screen whose openings are smaller than the smallest particle of the source.

The three main criteria used to evaluate a material as a chemical source are as follows:

1. Purity — The material should not release foreign vapors. A small amount could conceivably be tolerated in ordinary maser experiments if the vapors were not corrosive enough to affect the dimensions of the cavity. However, in a clock satellite experiment, where the ammonia would be pumped by a highly selective getter, the impurity level would have to be negligible over long periods of time.

2. Low heat of reaction — This feature is desirable in that as ammonia is released from a mass of the solid, the solid tends to cool somewhat and the temperature control problem becomes more difficult, the larger the heat of reaction for the evolution of the ammonia. This becomes even more of a problem when a large bulk of solid material is present as would be the case when long periods (several weeks) of continuous operation are required.

3. Pressure stability — The ammonia pressure should be independent of the degree of ammoniation and should remain constant under maser operating conditions where the ammonia supply would be depleted at the rate of the order of 10^{17} molecules/sec. This requirement practically eliminates purely physical adsorptive sources.

The material finally chosen for use as an ammonia chemical source was silver chloride-monoammoniate. The constant pressure of ammonia maintained over this material is translated into a constant ammonia flow to the maser by connecting a fine capillary from the chamber containing the ammonia gas in equilibrium with the solid to the maser. The capillary in this case consists of a 7-inch-length of stainless steel tubing with a bore of approximately 0.007 inch. The flow through such a capillary is given by

$$\text{Flow} = 2.5 \times 10^{27} \left(P_1^2 - P_2^2\right) \frac{r^4}{\ell T} \text{ molecules/sec}$$

where P_1 and P_2 ≡ the upstream and downstream pressure, respectively, in mm Hg

r ≡ radius of the capillary

ℓ ≡ length of the capillary

T ≡ absolute temperature.

Thus if the absolute temperature of the capillary is maintained constant within the required limits, we see that the flow through the capillary will, under typical operating conditions, remain constant.

Silver chloride-monoammoniate ($AgCl \cdot NH_3$) is a solid compound formed by the chemical combination of anhydrous silver chloride ($AgCl$) with gaseous anhydrous ammonia (NH_3)·$AgCl + NH_3 = AgCl \cdot NH_3$. A photograph of the apparatus for producing this material is shown in Fig. 12.

This low-molecular-weight (160 g/mol) low-vapor-pressure system thermostated and coupled to a simple capillary exhibits the following characteristics of an excellent solid-state source for ammonia beam masers:

1. The chlorine equilibrium vapor pressure above pure silver chloride at 25°C was calculated from its free energy of formation as 10^{-38} atmosphere.

2. Silver chloride is well known for its low affinity for water molecules and therefore is easily made anhydrous by low temperature bakeout.

3. The pressure of the ammonia gas over the $NH_3 - AgCl \cdot NH_3$ system, which is approximately 1/10 atmosphere at room temperature, remains constant at a given temperature as long as two phases are present. Therefore, the beam flow into the maser chamber remains constant until all of the ammonia is consumed.

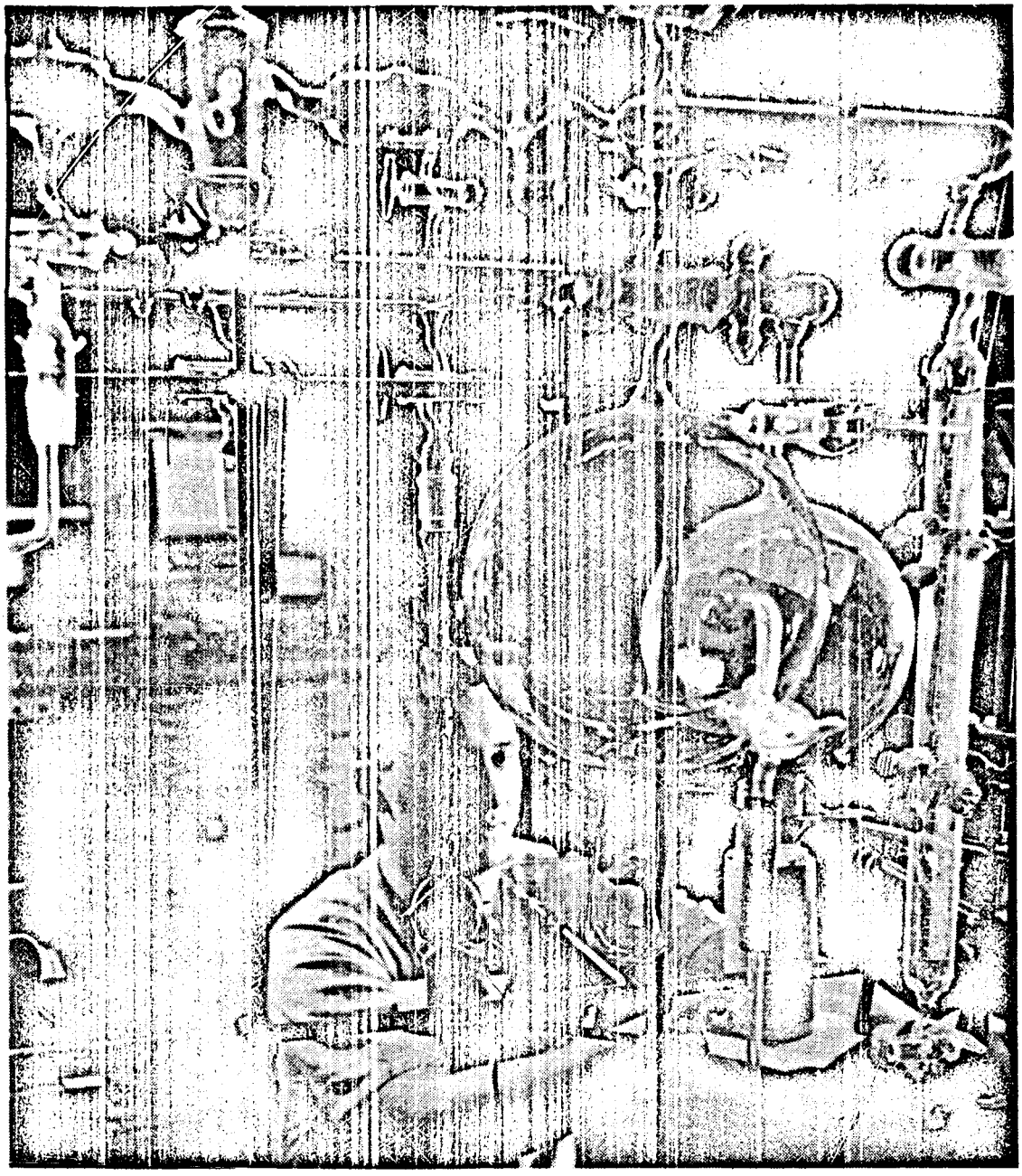

Fig. 12. Partial view of apparatus for preparation of chemical sources.

The source is prepared in a small copper sphere. On the outside of this sphere are located two closely coupled windings — a non-inductive, heater winding and a nickel wire temperature-sensing winding. The sensing winding, giving a large resistance change for a small change in temperature, constitutes one arm of a Wheatstone bridge. A ten-turn helipot located in one of the other arms sets the temperature to be maintained by the controller. This temperature controller is a narrow-band proportioning type which allows precise temperature control and maintains the temperature constant to $\pm 0.04^{\circ}C$. A photograph of the source container, capillary, and transistorized temperature controller is shown in Fig. 13.

That the source exhibits a constant vapor pressure independent of the degree of ammoniation has been verified by experiment. The change in equilibrium vapor pressure was followed with time by allowing the ammonia above the sample to pass through the capillary. In the first experiment, lasting 32 hours, the flow was observed, at steady state, to be stable within 0.42 percent; in a similar experiment in which a maser was operated continuously for 11 days, the flow was found to be stable within 5.5 percent. This is well within the requirements for operation of the ammonia beam maser with a frequency stability of one part in 10^{11}.

M 1931

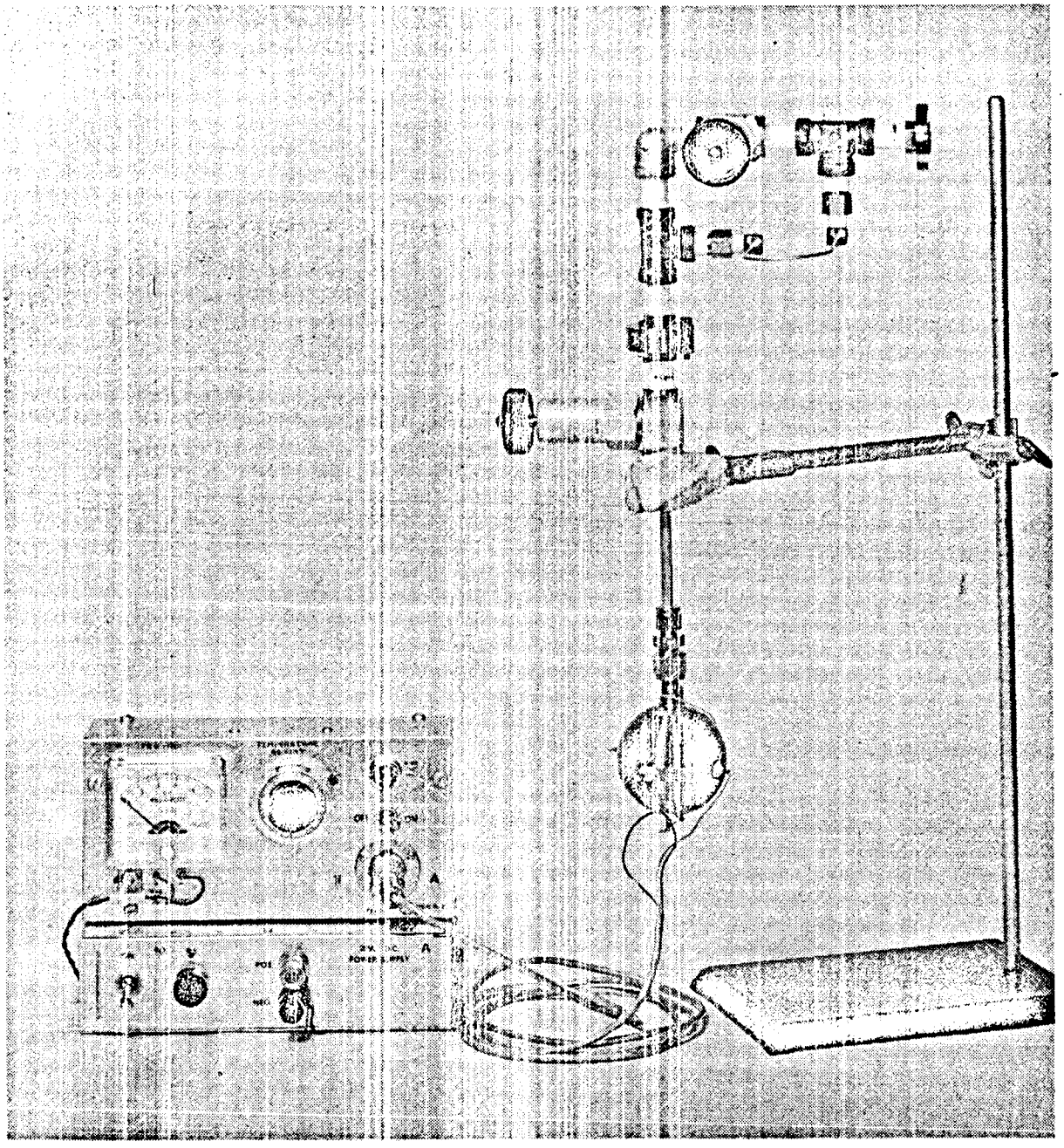

Fig. 13. Ammonia chemical source with the temperature control circuitry and capillary for regulation of ammonia flow.

VII. MASER PHASE-LOCKED TRACKING LOOP

The fact that the output signal of the ammonia maser with its high frequency stability occurs in the microwave region of the r-f spectrum and furthermore, is at an extremely low power level requires that one consider how to make best use of this stability, in particular, how it might be translated into a more usable frequency range and the available power increased. The technique employed here is one of multiplying the frequency of a 52.7-Mc crystal up to K-band and phase locking it to the maser signal by means of a phase-locked tracking loop.

The over-all loop can be represented by five major blocks as shown in Fig. 14. This is a fundamental feedback system which controls the frequency (ν_o) of the VCO with respect to the maser frequency(ν_m). Many frequencies, from very low values (< 1 Mc) up to K-band, are available from this loop, all with the long term stability of the maser.

The actual loop uses a double heterodyned I-F system with a phase detector controlling the VCO. It is apparent that the error which is detected by the phase sensitive detector will contain information from the reference frequency as well as from the signal. Similarly, instabilities of the translation frequency used to obtain the second intermediate frequency contribute to the error. Because of this, it is necessary to derive these two frequencies from the stable source. With this in mind, a new loop diagram can be drawn; see Fig. 15.

The relation of ν_m to ν_o is determined from this loop.

$$\frac{\nu_m}{\nu_o} = M + N(P + 1) = \text{constant},$$

where $M = 432$

$N = 1/4$

$P = 1/4$.

The expected drifts in the VCO during a satellite launch would be about one part in 10^8 per second. A loop bandwidth of 20 cps would be adequate to prevent loss of lock during this period; however, a further increase in this parameter is desirable to improve the short time stability of the VCO. The system, as does any feedback system, acts as a low-pass filter to noise associated with the input signal, but as a high-pass filter to any noise or jitter on the VCO frequency. The limitation on widening the loop bandwidth is the available signal-to-noise

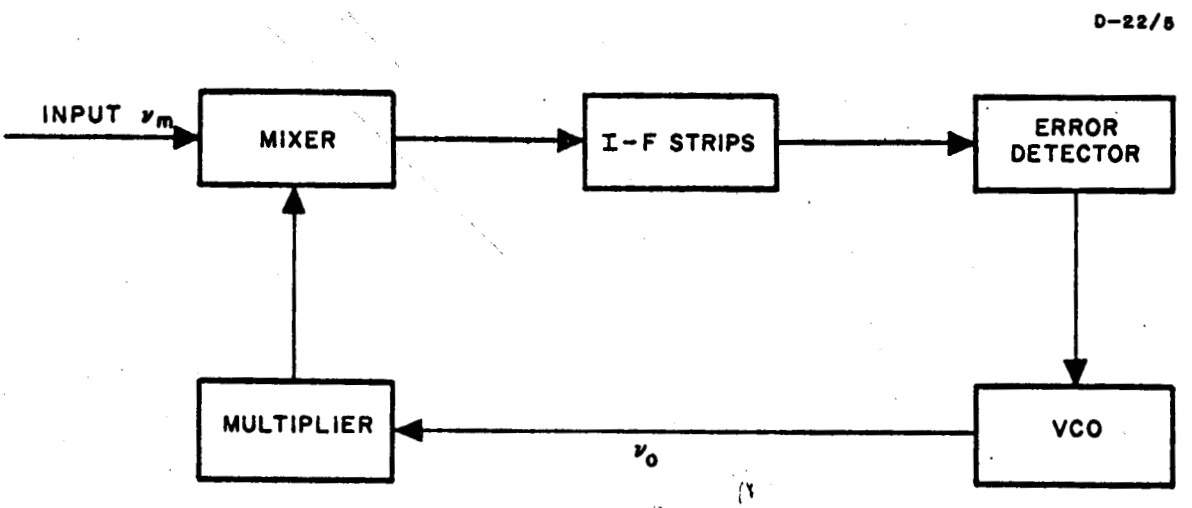

Fig. 14. Possible phase-locked tracking loop.

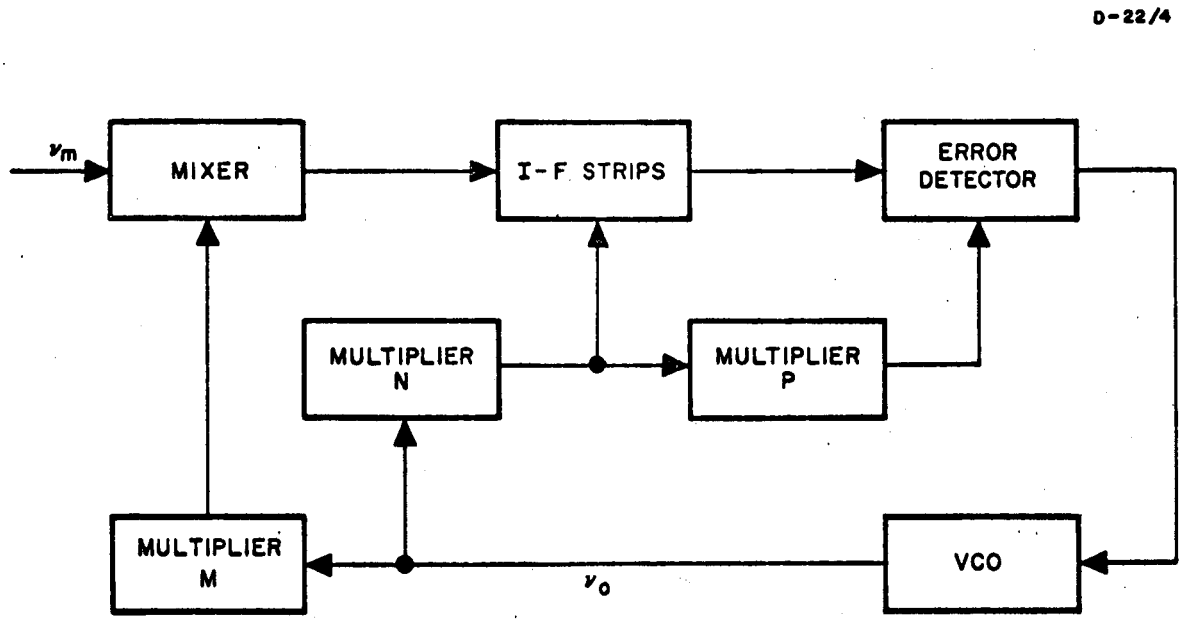

Fig. 15. Improved maser phase-locked tracking loop.

ratio. With an expected S/N of 17 db in a 20-kc-wide I-F strip, the loop tracking bandwidth was made 500 cps with a damping factor of 0.7. The tracking range of the system is 3 kc at the VCO frequency with an expected drift due to temperature of less than 500 cps.

To permit relock of the system in case of loss of track during launch or any phase of the operation, a discriminator function has been included. Whenever a frequency error or beat appears at the output of the phase detector which is outside the bandwidth of the tracking loop, a voltage of the proper polarity will be generated to reduce the frequency error and permit phase lock. The switching of the system from frequency control to phase control is inherent in the circuitry; no relays are needed. When the loop is phase locked, no voltage appears at the discriminator output and vice versa.

A detailed block diagram of this system is shown in Fig. 16, and a photograph of the system is shown in Fig. 17. A complete circuit diagram of the phase-locked loop is shown in Fig. 18. The function of the blocks is as follows:

Blocks 1, 2 and 3

The I-F amplifiers and mixer have an over-all gain of 110 db with a 3-db bandwidth of 20 kc. The first I-F amplifier uses five transistors and requires about 360 mw of power. Its gain is 80 db and, with the narrow-band crystal filter, is the bandwidth determining unit. The narrow-band filter, whose center frequency is 16.47 Mc, is placed between the first and second stages to reduce the incidence of noise-noise beats in the nonlinearities of the succeeding stages.

The second I-F amplifier, with a center frequency of 3.29 Mc, uses three transistors including the mixer and requires 180 mw of power. The gain of this amplifier is 30 db. The reason for such an apportionment of gain is to prevent leakage of the phase detector reference signal into the second I-F amplifier.

Blocks 4 and 5

The balanced mixer is a K-band mixer designed for operation at low power levels (-20 dbm). It uses a forward reverse pair of 1N26A crystals which are biased in the forward direction by a direct current of about 50 μa. The conversion gain is about -12 db.

Multiplication is obtained in multiplier M by the use of reactor diodes. The input power at the lowest frequency (ν_0 = 52 Mc) is approximately 700 mw. The technique used for multiplying separates naturally into two areas. The lower frequencies (from 52 to 2800 Mc) are

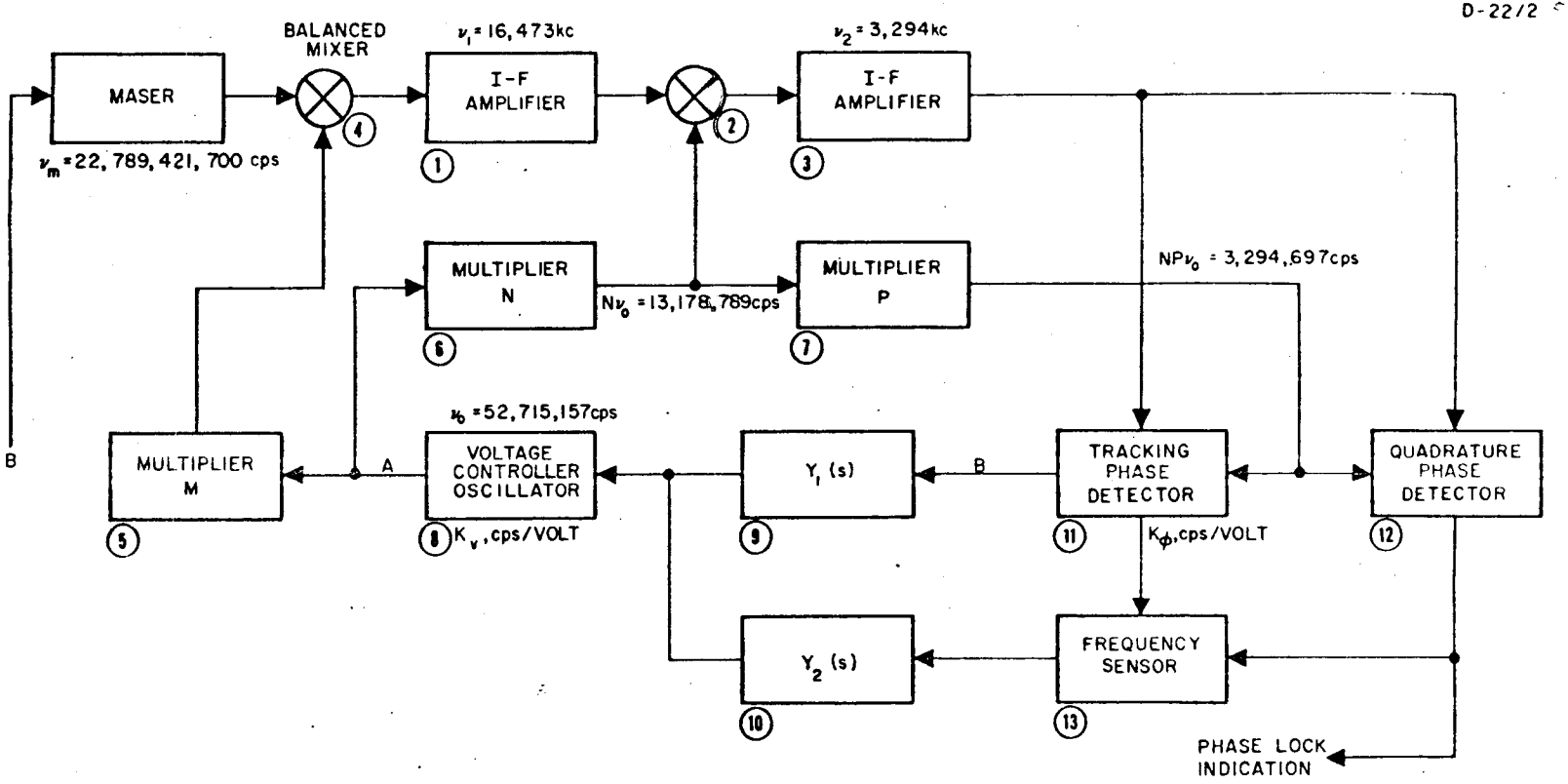

I-F BANDWIDTH = 20kc

M = 432

N = P = 1/4

$Y_1(s) = T_1 s + 1 / T_2 s + 1$

$$\nu_0 = \frac{\nu_1 + \dfrac{2\pi K_v K_\phi}{s}\left(\dfrac{T_1 s + 1}{T_2 s + 1}\right)\nu_m}{1 + \dfrac{2\pi K_v K_\phi \left[M + N(P+1)\right](T_1 s + 1)}{s(T_2 s + 1)}} \approx \frac{\nu_i}{1 + \dfrac{2\pi K_v K_\phi M (T_1 s + 1)}{s(T_2 s + 1)}}$$

POINT A: ν_i ADDED TO SIMULATE VCO DRIFT

POINT B: CONNECTIONS FOR MASER TUNING CIRCUITRY

Fig. 16. Complete diagram of the actual maser phase-locked tracking loop.

M 1930

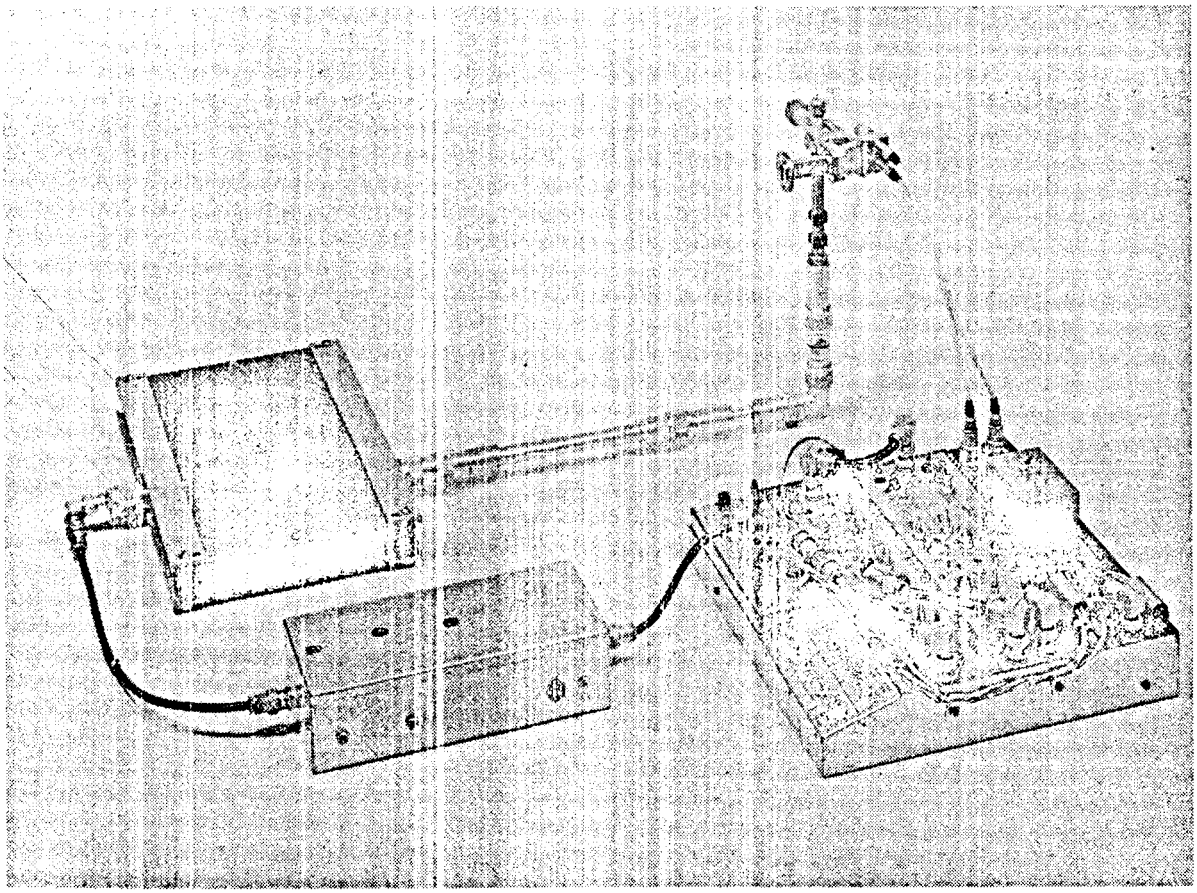

Fig. 17. Complete maser phase-locked loop. The maser signal input is one arm of the balanced mixer.

multiplied by using the variable reactive component of the reactor diodes. This portion of the chain includes three triplers and one doubler for a total factor of 54. The power level delivered at 2800 Mc is 15 mw. This signal drives the next part of the multiplier which uses the non-linear resistance characteristic of the reactor diode. The multiplying factor is eight, and the power delivered at 22.77 kMc is -20 dbm.

The total number of stages is five in the over-all chain. Initially two triplers using lumped parameter components develop 450 Mc. This section is followed by a tripler and a doubler using distributed parameter techniques in the form of a strip line. The last factor of eight involves the use of a coaxial system with a K-band waveguide output. The balanced mixer requires a drive of -20 dbm and a diode bias current of 50 μa and has a conversion gain of -12 db. Total power into the chain is about 1.3 watts.

Blocks 6 and 7

The multiplications N and P are identical. Each consists of two divide-by-two regenerative circuits and one buffer stage.

The first divider is driven with 52.7 Mc and delivers 13.2 to the I-F mixer and to the second divider which supplies the 3.29-Mc phase detector reference frequency. The two units consume a total of about 150 mw and require six transistors.

Block 8

The voltage-controlled crystal oscillator delivers approximately 250 mw of power into 50 ohms at 52.7 Mc to drive the main multiplier (block 5) and a small amount of power to the secondary multiplier (block 6).

The oscillator circuit uses one tetrode transistor with the crystal operated in its series mode feeding back from the collector to the emitter. Control of the frequency is obtained by varying the oscillator emitter current. The output impedance of the collector has a reactive component which is a function of emitter current and, as such, tunes the oscillator tank. This tuning introduces a change in the phase shift in the feedback loop and forces the crystal to operate at a different frequency, one which compensates for the introduced phase shift. A sensitivity of 2500 cps/ma of the emitter current, I_e, is available by this method. Initial adjustment of the oscillator frequency will be made by proper tank tuning and with a current control in the emitter of the oscillator stage. A high sensitivity to control voltage required operation of the oscillator at low power output and necessitated the use of two class B amplifier stages. The total power into the voltage controlled oscillator is 650 mw.

Blocks 9 and 10

These two blocks are passive circuits to provide the proper parameters for the loop performance. The unit in the phase loop is a lead-lag or pole and zero circuit, while the one in the frequency loop is merely a low-pass filter or single-pole circuit.

Blocks 11 and 12

The phase detectors used in this system are the diode type driven by transformers. Block 11 and block 12 differ only in that the signal from the I-F amplifier is applied to one of the circuits 90 degrees out of phase from that applied to the other circuit.

Each circuit uses two transistors, one to amplify the reference signal for the phase detector transformer and one to reduce the loading of the phase detector on the I-F amplifier. Total power is about 250 mw.

The outputs of the phase detectors provide signals to the frequency sensing circuit, the main tracking error signal and the lock indication voltage.

Block 13

The frequency sensor is used to permit relock of the loop in the event that loss of phase lock does occur. The circuit is designed to give outputs for frequencies beyond the pull in range of the phase loop.

Its operation is as follows: When the loop is not tracking, a beat frequency equal to the difference between the signal and the reference frequencies will appear at the output of the two phase detectors. The output signals from the phase detectors have the characteristic that the relative phase of the two signals will reverse when the relative magnitudes of the signal frequency and the reference frequency reverse. That is, the quadrature phase detector output will lead the tracking phase detector output by 90 degrees when the signal frequency is below the reference frequency. This information is extracted by the frequency sensing circuits and provides a voltage of a polarity which will reduce the frequency error.

The circuitry requires four transistors and about 120 mw of power.

VIII. TUNING PROCEDURE FOR MASER CAVITY

As discussed earlier, the stability of the maser signal is affected by the tuning of the microwave cavity system to a degree which necessitates precise adjustment of this device. Fortunately, a phase-locked system provides a means to detect small effects in the signal due to misalignment. It is possible to detect any low frequency modulation that is present on the maser signal with a modulation index of approximately 0.002 or greater.

It has been shown[3] that the amount of frequency modulation capable of being induced on the maser signal is a function of cavity detuning. The technique used here will be to frequency modulate the spectral line of the output with a magnetic field (Zeeman effect). The frequency of the modulation, which is twice the driving frequency since a magnetic field in either direction produces a frequency shift, is chosen such that it is within the tracking bandwidth of the phase-locked tracking loop. Within its bandwidth the loop can follow any perturbations on the input signal; as a result, the frequency of the modulation will appear on the output of the tracking phase detector. This signal, along with any jitter, noise, or other variations, is fed into a correlator which extracts the frequency of the modulation. The output of the correlator is a d-c voltage which has a magnitude proportional to the modulation index of the f-m for small modulation indices (< 0.3). The cavity is then tuned in such a way as to minimize this modulation index. A block diagram of the system is shown in Fig. 19.

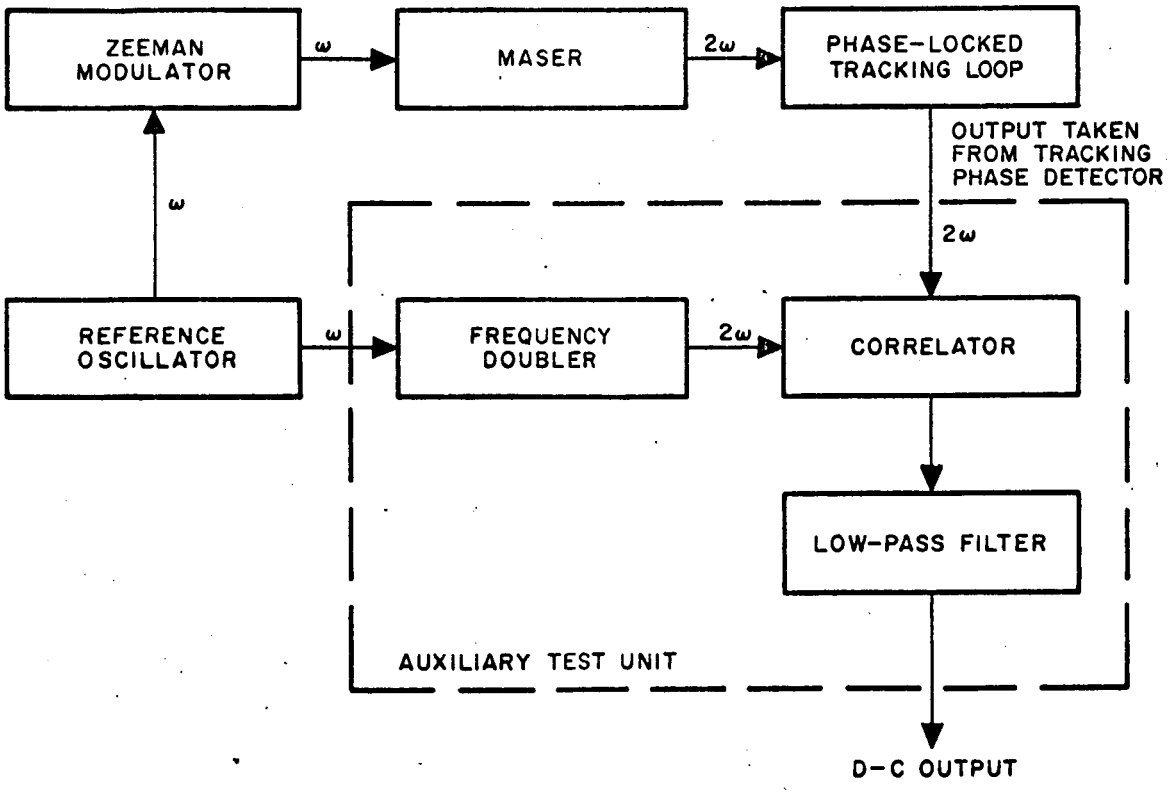

Fig. 19. Block diagram of setup for detecting frequency modulation of the maser signal.